Self-Assembly of a Fluorocarbon−Hydrocarbon Hybrid Surfactant: Dependence of Morphology on Surfactant Concentration and Time

Yutaka Takahashi,[†,‡] Yukishige Kondo,*[,†,‡] Judith Schmidt,[§] and Yeshayahu Talmon*[,§]

Department of Industrial Chemistry, Faculty of Engineering, Tokyo University of Science, 12-1 Ichigaya-Funagawara, Shinjuku, Tokyo 162-0826, Japan, Center for Colloid and Interface Science (CCIS), Tokyo University of Science, 1-3 Kagurazaka, Shinjuku, Tokyo 162-8601, Japan, and Department of Chemical Engineering, Technion-Israel Institute of Technology, Haifa 32000, Israel

Received: March 29, 2010; Revised Manuscript Received: August 4, 2010

The morphologies of aggregates formed from a hybrid surfactant (F6H5OS) whose molecules have a hydrocarbon chain (pentyl group) and a fluorocarbon chain (perfluorohexyl group) were studied along with changes in the morphologies with time. F6H5OS exhibits a micelle−vesicle transition at a concentration of 5.5 mM in water. Cryo-TEM observation of 5 mM aqueous F6H5OS solution reveals the existence of only micelles with a diameter of ca. 6 nm, while the coexistence of micelles and vesicles is observed in 10 mM aqueous F6H5OS solution. When the 10 mM aqueous F6H5OS solution is aged, the micelles are transformed into vesicles. Further, the vesicles have different structures, namely, spherical and tubular structures. ^{1}H NMR, ^{1}H−^{1}H NOESY, and FT-IR experiments suggest that upon aging, the conformation of hydrocarbon chains in F6H5OS changes, and the hydrocarbon chains are located close to the phenyl group in the surfactant molecules. At concentrations above 5.5 mM, small micelles are formed immediately after the preparation of the F6H5OS solutions; those micelles subsequently transform into vesicles. The hybridity of F6H5OS, i.e., having a fluorocarbon chain and a hydrocarbon chain in its molecule, plays an important role in the transformation of micelles into vesicles upon aging.

Introduction

The surfactants of amphiphilic molecules form organized aggregates of different shapes and sizes in their aqueous solutions above critical aggregation concentrations. The morphologies of the aggregates, e.g., spherical micelles, threadlike micelles, vesicles, and lamellar bilayers, depend primarily on the molecular structure of the surfactants. Studies of the morphological transition of aggregates could be of great importance for various applications. For example, these changes often bring about changes in the viscosity of the surfactant solutions, and the surfactant aggregate morphology can be used as a template for structured inorganic materials. It is well-known that the morphological transition of surfactant aggregates may be caused by the addition of additives[1−3] or the variation of solution conditions such as the surfactant concentration,[4,5] pH,[6,7] and temperature.[8,9] We have also reported that the addition of sodium dodecylsulfate (SDS) to lamellar aggregates formed from didodecyldimethylammonium bromide (DDAB) leads to spontaneous vesicle formation.[10] In addition, transitions have also been achieved by applying external forces such as shear[11,12] and stirring[13] to surfactant solutions. However, there are few studies on the gradual transformation of micelles to vesicles.[14] As described below, morphological changes in surfactant aggregates might be brought about by the nature of hybrid surfactants, that is, by the intramolecular coexistence of fluorocarbon (FC) and hydrocarbon (HC) chains, which are mutually immiscible.

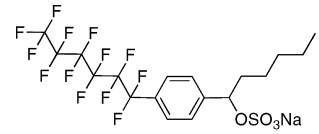

F6H5OS

Y. Kondo's research group has been involved in the synthesis of various types of amphiphiles that possess a FC chain and a HC chain. Such amphiphiles are referred to as *hybrid surfactants*,[15−18] and their unique solution properties, such as the emulsification of ternary mixtures of HC oil/FC oil/water,[18] intramicellar phase separation between the FC and HC chains,[19] and the unusually long lifetime of the micelles, have been reported by Kondo's group.[20]

Here, we report the morphology of aggregates formed of a sulfate salt-type hybrid surfactant (F6H5OS) in water and describe morphological changes upon aging the surfactant solutions. We use cryogenic transmission electron microscopy (cryo-TEM), electrical conductivity measurements, and pulsed-gradient spin echo nuclear magnetic resonance spectroscopy (PGSE-NMR) to study the surfactant solutions. In addition, we suggest a new mechanism to explain how the conformation change in alkyl chains in the surfactant brings about a significant change in its morphology.

Experimental Section

Materials and Sample Preparation. Sodium 1-[4-(perfluorohexyl)phenyl]-1-hexyl sulfate (F6H5OS) was synthesized by the method reported in a previous paper.[21] Surfactant solutions were prepared in high-purity H_2O (Milli-Q pure water; $R = 18$ MΩ cm, $\gamma = 72.8$ mN/m at 25 °C) and stored at 30 ± 0.1 °C.

* To whom all correspondence should be addressed. E-mail: (Y.K.) ykondo@ci.kagu.tus.ac.jp, (Y.T.) ishi@tx.technion.ac.il.

† Department of Industrial Chemistry, Tokyo University of Science.

‡ Center for Colloid and Interface Science (CCIS), Tokyo University of Science.

§ Technion-Israel Institute of Technology.

10.1021/jp1028273
Published on Web 09/30/2010

Measurements were carried out after the samples had been stored for 3 h or more. Depending on the storage period, these samples are referred to as fresh and aged solutions.

Electrical Conductivity Measurements. The electrical conductivity of aqueous surfactant solutions prepared using H_2O were measured at 30 °C with a CM-60G conductivity meter (DKK-TOA, Tokyo, Japan) equipped with a CT-57101B electrode (DKK-TOA). Concentrations used in this experiment ranged from 1.0 mM (above the critical micelle concentration) to 20 mM.

Light Microscopy. Differential interference contrast (DIC) microscopy was performed with a Leica DMI 4000B microscope (Leica Microsystems GmbH, Wetzlar, Germany) at room temperature (rt). Digital images of samples were captured using a Leica DFC300 FX digital camera.

Cryo-TEM Observations. Cryo-TEM was performed with an FEI T12 microscope. Vitrified samples were prepared in a controlled environment vitrification system (CEVS) at 30 °C and 100% relative solvent saturation. A drop of the solution to be imaged was placed on a perforated carbon film supported on an electron microcopy Cu grid, held by the CEVS tweezers. The sample was blotted by a filter paper and was immediately plunged in liquid ethane at its freezing point (−183 °C). The vitrified specimens were then stored under liquid N_2, transferred to a Gatan 626 cooling holder via its "workstation", and imaged in the TEM microscope at about −180 °C. Images were recorded at an acceleration voltage of 120 kV in the low-dose mode to minimize electron-beam radiation damage.

NMR Measurements. The NMR techniques employed in this study were 1D ^{1}H NMR, PGSE-NMR, and ^{1}H−^{1}H nuclear Overhauser enhancement spectroscopy (NOESY). NMR measurements of 2.0 and 10 mM aqueous F6H5OS solutions were carried out at 30 °C on a Bruker Avance DPX-400 spectrometer, equipped with a QNP probe operating at 400 MHz for ^{1}H nuclei. All samples were prepared using D_2O (Acros Organics; 99.8 atom %D) as the solvent. The ^{1}H NMR chemical shifts of the surfactant were determined by the 7.260 ppm signal for a trace amount of $CHCl_3$ in $CDCl_3$ (Acros Organics; 99.8 atom %D) as the external standard.

PGSE-NMR measurements of ^{1}H nucleus were carried out at 30 °C with D_2O lock. The gradient pulse width (δ) and diffusion delay (Δ) were 2 and 200 ms for 2.0 mM surfactant solutions, respectively; the values were 2 and 400 ms for 10 mM surfactant solutions, respectively. The spin echo intensity (I_g) was measured as function of the gradient strength (g). Using the nonlinear least-squares method, the diffusion coefficient of F6H5OS (D_s) in D_2O was estimated from the following equation:

$$I_g = I_0 \exp[-\gamma^2 g^2 \delta^2 D_s(\Delta - \delta/3)] \quad (1)$$

where γ is the gyromagnetic ratio of the ^{1}H nucleus and I_0 is the spin echo intensity at $g = 0$.[22] Before the measurements, g was calibrated using the diffusion coefficient of a trace amount of H_2O in D_2O, D ($= 1.902 \times 10^{-9}$ m^2 s^{-1}).[23] In this study, the D_s value was determined by the ^{1}H NMR signal of the ω-CH_3 group in F6H5OS. If the monomer concentration of the surfactant remains constant above the critical micelle concentration (cmc), the D_s value gives a single weight-average signal for the surfactants in both states of monomer and aggregate. The diffusion coefficient of aggregates (D_{agg}) can be expressed as:

$$D_{agg} = \frac{1}{p_{agg}} D_s - \frac{p_{mon}}{p_{agg}} D_{mon} \quad (2)$$

where p_{agg} and p_{mon} are the mole fractions of surfactants in monomer and aggregate states, respectively, and D_{mon} is the diffusion coefficient of the surfactant monomer, equal to D_s below the cmc. Finally, hydrodynamic radii of the F6H5OS aggregates were calculated from the D_{agg} values estimated using the Stokes−Einstein equation. ^{1}H−^{1}H NOESY experiments were performed for a mixing time of 1.0 s at 30 °C.

FT-IR. FT-IR measurements were performed with JASCO FT/IR-6000 spectrometer at room temperature. Surfactant solutions were prepared using D_2O as a solvent. A demountable liquid cell with CaF_2 windows was employed for the measurements.

Results and Discussion

Aggregates in Fresh Solutions. First, we present the morphology of aggregates formed by F6H5OS in fresh solutions. The electrical conductivity of aqueous surfactant solutions was measured at different concentrations. The conductivity increased linearly with the concentration, up to 5.5 mM, and the slope of the conductivity vs concentration line changed abruptly beyond 5.5 mM (Figure 1). In addition, the average diffusion coefficient, D_{agg}, of aqueous F6H5OS solutions decreased beyond 5.5 mM, indicating the formation of large aggregates (Figure S1, Supporting Information). F6H5OS forms micelles in water above 0.30 mM (critical micelle concentration),[20] and hence the break in the slope of the conductivity vs concentration line and the decrease in the D_{agg} values indicate the transition to larger aggregates formed by F6H5OS in aqueous solutions. When the 2.0 mM fresh F6H5OS solution was observed by light microscopy, no aggregates were observed. In light microscopy, aggregates with a diameter as large as ca. 1 μm can be observed. That implies that the diameter of most of the aggregates formed by F6H5OS was less than 1 μm. Figure 2 shows a cryo-TEM image of a 5.0 mM fresh F6H5OS solution. A number of spherical and spheroidal micelles with a diameter of ca. 6 nm are observed (for example, see the arrows).

In contrast, light microscopy of a 10 mM fresh F6H5OS solution revealed the formation of vesicles with diameters of a few micrometers to 30 μm (arrows in Figure 3). Considering that micelles and vesicles were observed at concentrations of 5.0 mM and 10.0 mM, respectively, the inflection point (5.5 mM) seen in the conductivity experiment corresponded to the concentration, at which the micelle−vesicle transformation occurs. When 10 mM solution is compared to 5 mM solution by the naked eye, 10 mM solution was slightly turbid, whereas 5 mM solution was transparent. Figure 4 shows cryo-TEM images of 10.0 mM fresh solutions. We observe small vesicles with diameters of 20 to 70 nm coexisting with some micelles (Figure 4a). The surfactant also formed larger vesicles with diameters of 400 nm to 1 μm, some containing smaller vesicles (Figure 4b).

Aggregates in Aged Solutions. Figure 5 shows the time dependence of the electrical conductivity of 2.0 mM and 10 mM aqueous F6H5OS solutions at 30 °C; the concentrations of the two solutions are below and above the transition point (5.5 mM), respectively. The conductivity of the 2.0 mM F6H5OS solution hardly changed with time. However, the conductivity of the 10.0 mM solution decreased with time up to 40 days after its preparation.

In general, the electrical conductivity of aqueous ionic surfactant solutions is strongly affected by the concentrations

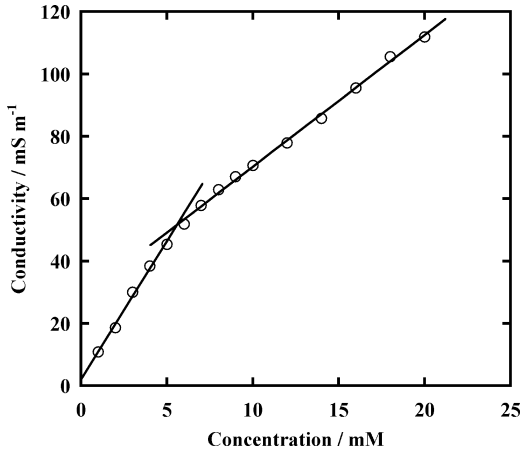

Figure 1. The relation between the electrical conductivity of fresh aqueous F6H5OS solutions and surfactant concentrations.

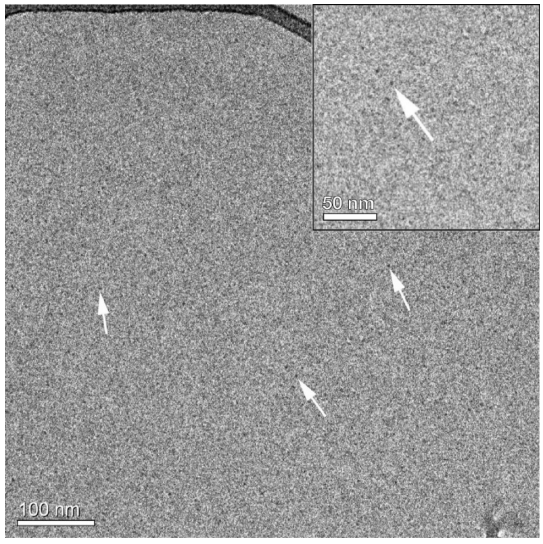

Figure 2. Cryo-TEM image of 5 mM fresh F6H5OS solution.

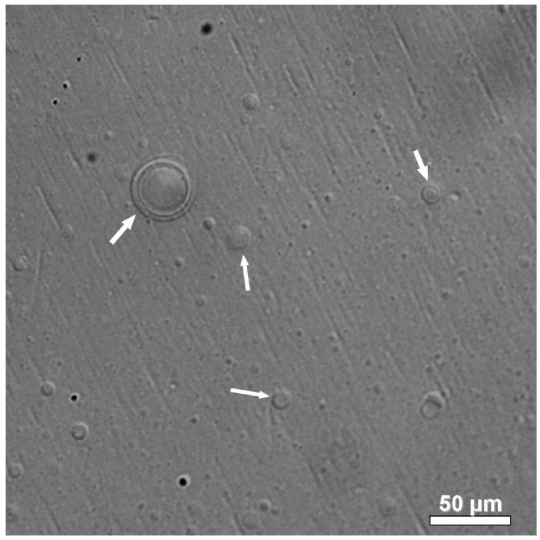

Figure 3. DIC microscopy image of 10 mM fresh F6H5OS solution.

of free counterions and free surfactant monomers.[24] According to the critical packing theory, the smaller the cross-section area of the hydrophobic−hydrophilic interface in the surfactant, the larger the critical packing parameter (CPP) of the surfactant molecule, defined by the equation CPP = v/al (v: volume of the hydrophobic chain, a: cross-section area of the hydrophobic−hydrophilic interface, l: fully stretched length of the hydrophobic chain), the smaller the curvature of aggregates formed from the ionic surfactant in water. A decrease in the conductivity of the 10 mM solution with time may indicate the decrease in the free counterion concentration and the resultant decrease in the effective size of the headgroup in the F6H5OS molecule, which leads to the reduction of the value a and subsequent increase in the CPP. In other words, the decrease in the conductivity may suggest that large aggregates with small curvatures are continuously formed with time. If this hypothesis is correct, we should be able to observe an increase in the average diameter, or a decrease in the average aggregate diffusion coefficient, D_{agg}, for the 10 mM solution with the passage of time up to 40 days after the preparation of the solution.

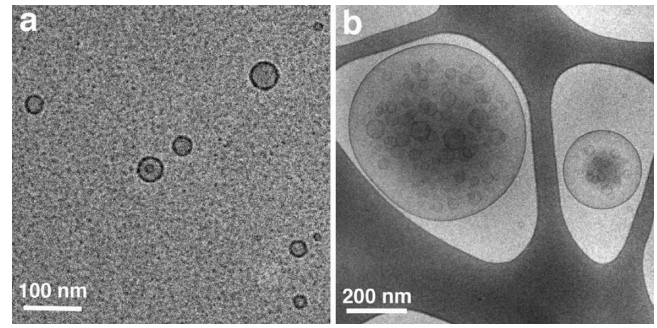

Figure 4. Cryo-TEM images of 10 mM fresh F6H5OS solutions. The dark areas in Figure 4b are the support film.

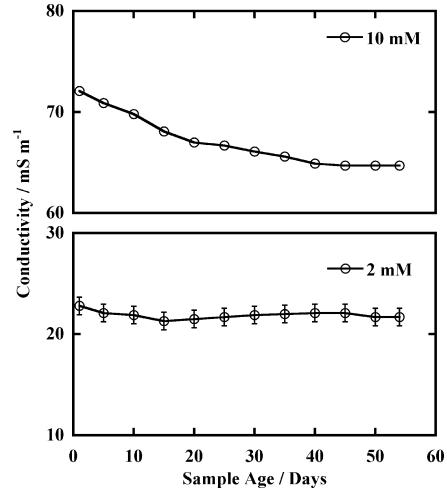

Figure 5. Change in the electrical conductivities of 2 mM and 10 mM aqueous F6H5OS solutions at 30 °C with time.

Figure 6a shows the D_{agg} values for a 2.0 mM aqueous F6H5OS solution, measured by PGSE-NMR, as a function of time. D_{agg} for the fresh solution, which is a surfactant solution equilibrated at 30 °C for 3 h after preparation, was 7.823×10^{-11} m^2 s^{-1}. The diameter of the aggregates calculated by the Stokes−Einstein equation was ca. 6 nm, consistent with the micellar size observed by cryo-TEM (see Figure 2). D_{agg} and the diameter of the aggregates were almost constant with an increase in time until 55 days after preparation. Thus, the morphology of the micelles formed in the 2.0 mM F6H5OS solution hardly changed with time. PGSE-NMR measurements were also performed at different times for the 10 mM aqueous surfactant solution. As seen in Figure 6b, D_{agg} of the solution monotonously decreased with an increase in time and reached a constant value after 40 days. In other words, the average diameter of the aggregates formed in the 10 mM F6H5OS

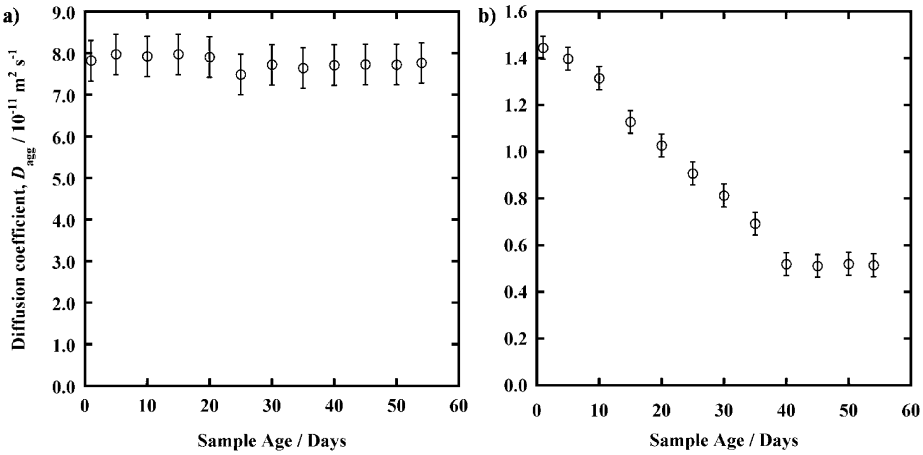

Figure 6. Change in the diffusion coefficients of aggregates (D_{agg}) in 2 mM and 10 mM aqueous F6H5OS solutions with time after the preparation of the solutions. (a) 2 mM, (b) 10 mM.

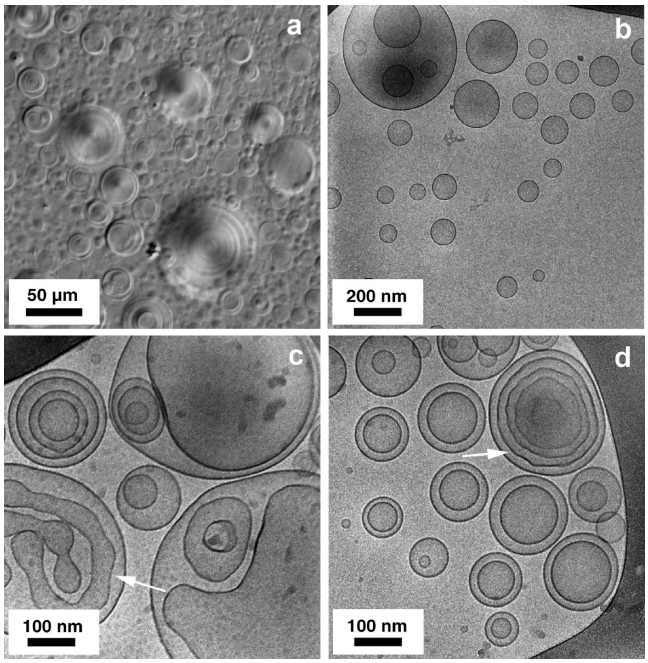

Figure 7. DIC light microscopy and cryo-TEM images of 10 mM aqueous F6H5OS aqueous solutions 53 days after the preparation of the solutions. Note in c that an arrow points to a tubular vesicle encapsulated inside a spherical one; in d the membranes show faceting. The polyhedral appearance may be the result of the confinement of vesicles within vesicles.

solution increased upon aging the solution and reached a constant value after 40 days. Note that the conductivity (Figure 5) also became constant 40 days after preparation. Thus, the morphology of aggregates formed in the 10 mM solution stabilizes upon aging the solutions over more than 40 days at 30 °C.

Figure 7 shows a DIC micrograph and cryo-TEM images of 10 mM F6H5OS solutions 53 days after their preparation. The DIC image (Figure 7a) shows many giant vesicles and multilamellar vesicles. Considering that few vesicles were observed in the 10 mM fresh F6H5OS solutions by DIC microscopy (see Figure 3), the aging of the solution seems to generate many vesicles. The cryo-TEM images of the aged solutions also indicate the existence of many vesicles. The size and number of vesicles in an aged solution were larger than those in a fresh solution. As can be seen in Figure 7b, vesicles coexisted with small micelles; however, the number of micelles was smaller than that in the fresh solution. Indeed, the aging of the solutions leads to the transformation of the micelles into vesicles.

Possible Mechanisms of Transformation from Micelles to Vesicles. Past studies of the self-assembly of surfactants or polymers with FC, HC, and hydrophilic parts (segments) have found that these molecules form aggregates in which three segregated domains, FC domain, HC domain, and hydrophilic domain, coexist.[25,26] This is because each part (segment) is mutually immiscible with the other parts. Previously we studied another FC−HC hybrid surfactant (F6H4S), structurally analogous to F6H5OS. We observed that the surfactant formed in water micelles, in which the FC chains formed the micellar core, and the HC chains were excluded from the micellar core to the micellar surface by the self-assembly of FC chains. In the present study, F6H5OS was observed to form micelles at concentrations lower than 5.5 mM. Similar to F6H4S in the previous study, it is possible that the FC chains in F6H5OS formed the micellar core, while the HC chains were located on the micellar surface (Scheme 1).

The critical packing parameter (CPP) of a surfactant is an important parameter that determines the morphology of surfactants in aqueous solutions.[27] Single-chain surfactants in aqueous dilute solutions have CPP < 1/3 and therefore form spherical or spheroidal micelles. Considering that F6H4S forms spheroidal micelles, and the FC chains in F6H4S form the micellar core, it is reasonable to consider that F6H5OS also behaves like a single-chain surfactant in dilute solutions and forms micelles. In the process of micelle formation, the FC chain plays the role of a hydrophobic chain, and the HC chain is expelled to the micellar surface. There may exist hydrophobic interactions between the HC chains, and the HC chains may be self-assembling in the close proximity of the micellar surfaces.

In the case of ionic surfactants, an increase in concentration brings about an increase in their CPP, since the effective size of the hydrophilic group in the surfactants decreases with an increase in the ionic strength of the solution. The increase in the CPP causes the formation of large aggregates with a low curvature, such as threadlike micelles and lamellae (vesicles) formed from micelles. In this study, the transformation from micellar solution to lamellar phase (vesicular solution) containing micelles was seen at 5.5 mM. The vesicle formation at high concentrations, that is, above 5.5 mM, is consistent with the CPP theory.

However, the increase in the number of vesicles upon aging the 10 mM solutions in which vesicles and micelles coexist is

SCHEME 1: Micelle and Vesicle Formation by F6H5OS[a]

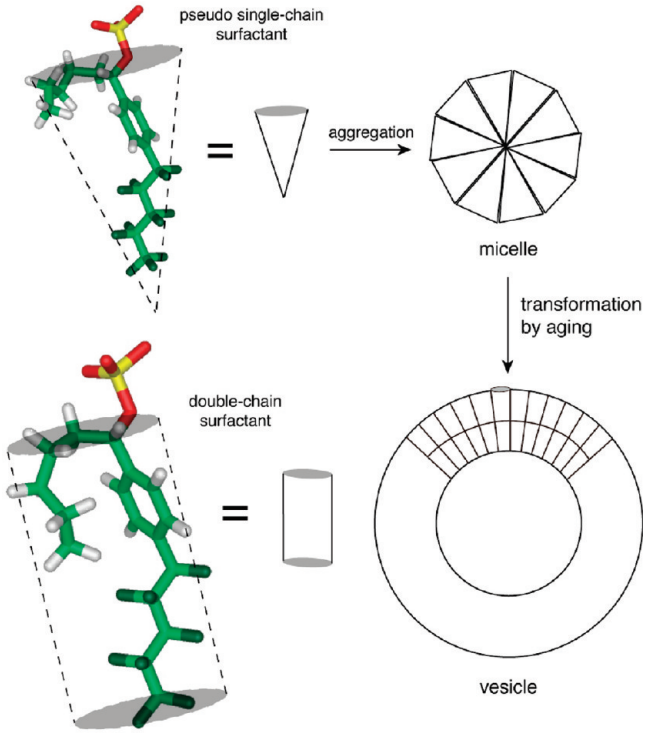

[a] The surfactant behaves as a pseudo-single-chain surfactant, and FC chains comprise the micellar core. FC chains, HC chains, and hydrophilic groups would be mutually segregated in the micelle. Vesicles are formed at solution concentrations above 5.5 mM at 30 °C. The surfactant tends to form micelles immediately after the preparation of the solutions, and subsequently, with aging, micelles gradually transform into vesicles. In the vesicles, the ω-CH_3 group (H1) and some methylene units (H2) in the surfactant are located close to the phenyl group, which leads to correlations between the phenyl protons and the H1, and between the phenyl protons and H2 protons in the 2D $^1H-^1H$ NOESY spectrum (see Figure 8).

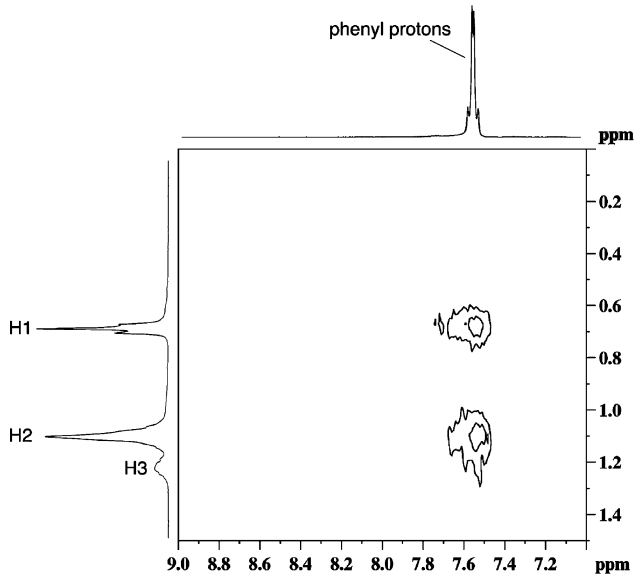

Figure 8. Contour plots constructed from data obtained in the 2D $^1H-^1H$ NOESY experiment involving the use of 10 mM aged F6H5OS solution (solvent: D_2O) at 30 °C.

yet to be explained. Upon comparing the cryo-TEM image of the 10 mM F6H5OS solution recorded 53 days after preparation to that obtained just after preparation, we clearly observe that the number of micelles is smaller in the aged solution. This indicates that micelles in the 10 mM solution were transformed to vesicles with time.

TABLE 1: Chemical Shifts for ^1H Nuclei in the Alkyl Chain of F6H5OS in Fresh and Aged (53 days after preparation) Solutions

	chemical shift, δ/ppm		
protons[a]	fresh soln	aged soln	$\Delta\delta$[b]
H1	0.6856	0.6817	−0.0039
H2	1.1035	1.1030	−0.0005

[a] $CF_3(CF_2)_5$–C$_6$H$_4$–OSO_3Na–$CHCH_2CH_2(CH_2)_2CH_3$ (H3, H2, H1)

[b] $\delta_{aged} - \delta_{fresh}$.

NMR chemical shifts are sensitive to the environment of the nuclei, which leads us consider the conformation and structural properties of aggregates. Table 1 presents the ^1H NMR chemical shifts for HC chains in 10 mM fresh F6H5OS solution and 10 mM aged F6H5OS solution (solvent: D_2O). The chemical shift for β-protons (H3) is not shown in the table, because the NMR signal of H3 is broad. The chemical shifts for the ω-CH_3 (H1) group and for six protons belonging to three methylene units (H2) move upfield upon aging the solution. This is thought to be due to the magnetic shielding of the H1 and H2 nuclei by the phenyl group or by the ^{19}F nuclei of the FC chain,[28] indicating that the ω-CH_3 group is located close to the phenyl group or FC chain in F6H5OS, when the surfactant solution is aged.

To consider the conformation of the HC chain in F6H5OS in greater detail, $^1H-^1H$ NOESY measurements were performed for 10 mM fresh solution and 10 mM solution aged for 53 days. Figure 8 shows the contour plots for the 10 mM aged solution obtained using data acquired in the NOESY experiments at 30 °C. The one-dimensional (1D) NMR signal around 7.5 ppm corresponds to the four phenyl protons in F6H5OS. It can be seen in the figure that there is a correlation between phenyl protons and H1 protons and between phenyl protons and H2 protons, indicating that the phenyl protons and H1 protons (ω-CH_3 group) and the phenyl protons and H2 protons are separated by a distance lesser than about 0.5 nm. In other words, the alkyl chain in the surfactant is in close proximity to the phenyl group. However, there is no correlation between phenyl protons and H1 protons (ω-CH_3 group) for the 10 mM fresh F6H5OS solution (Figure S2, Supporting Information).

In addition, preliminary FT-IR measurements were performed for a 10 mM fresh F6H5OS solution and a 10 mM aged F6H5OS solution (53 days after preparation), both of which were prepared by using D_2O as the solvent. The peaks corresponding to the CH symmetric stretching mode (ν_s^{CH}) and the CH asymmetric stretching mode (ν_{as}^{CH}) are known to shift to higher wavenumbers with an increase in the number of gauche conformers in the alkyl chains.[29,30] In the fresh solution, ν_s^{CH} and ν_{as}^{CH} appeared at 2856 and 2922 cm^{-1}, respectively. In contrast, for the aged solution, the modes were observed at 2861 and 2927 cm^{-1}, respectively. It is thought that the aging of the surfactant solution causes an increase in the number of gauche conformers in the HC chain of F6H5OS.

Combining the NMR chemical shift, the results of the NOESY and IR experiments, and the fact that the hybrid surfactant F6H4S considered in the previous study forms aqueous micelles with a core mainly consisting of FC chains, we postulate the following mechanism for the change in the morphologies of F6H5OS aggregates. As shown in Scheme 1,

at concentrations lower than 5.5 mM, F6H5OS molecules aggregate into small spherical or spheroidal micelles in which FC chains are preferentially packed into the core of the micelle, and the HC chains are located close to the micellar surface, because of their immiscibility with FC chains. Since FC chains are more hydrophobic than HC chains, and since FC and HC chains are mutually immiscible, FC chains are more likely to form the micellar core than HC chains. In dilute solutions, the surfactant molecules behave as a pseudo-single-chain surfactant, and the HC chain does not act as a hydrophobic chain. As can be seen in Scheme 1, the HC chain expelled by the FC chains may physically increase in the cross-section area (a) of the hydrophobic−hydrophilic interface in the surfactant, decreasing the CPP value, and make the shape of F6H5OS molecule conical. Conical surfactants should favor micelles being formed. Increase in the surfactant concentration leads to an increase in the ionic strength of the aqueous solution, and subsequently brings about a decrease in the effective size of the hydrophilic group (sulfate anion) in F6H5OS. This triggers the transformation of small micelles into larger aggregates with a small curvature, that is, lamellae (vesicles). Indeed, the electrical conductivity of aqueous F6H5OS solutions containing 10 mM NaCl (solvent having a high ionic strength) increased linearly with the surfactant concentration up to 0.8 mM and the slope of the conductivity vs concentration line changed beyond 0.8 mM, less than 5.5 mM, which supports that the increase in the ionic strength triggers the transformation of small micelles into larger aggregates (Figure S3, Supporting Information). During the transformation, the penetration of the HC chains located close to micellar surfaces into the aggregates facilitates the transformation of micelles to large aggregates (vesicles) with a small curvature (Scheme 1), because of the increased chain volume, v, leading to an increase in the CPP. HC chains are essentially hydrophobic, and therefore HC chains inside vesicle bilayers may be thermodynamically more stable than those located around micellar surfaces. The HC chains close to the surface are forced to come into contact with water and therefore are thermodynamically unstable. As mentioned above, the 10 mM solution aged for 53 days after preparation contains many vesicles, and the ω-CH_3 group and H2 protons are positioned close to the phenyl group in the surfactant. This means that F6H5OS molecules function as double-chain surfactant molecules.

As seen in Figures 5 and 7, the solution properties, such as electric conductivities and diffusion coefficients, of the 10 mM solution stabilized 40 days after preparation. In addition, it was observed that the number of micelles decreased and the number of vesicles increased upon aging the solution. Just after the preparation of the solution, the surfactant molecules favorably aggregated to form micelles with a core consisting of FC chains; the FC chains formed the core, owing to their stronger hydrophobicity as compared to the HC chains. In other words, F6H5OS kinetically forms micelles in the 10 mM solution immediately after the preparation of the solution. However, aging makes the solution thermodynamically stable, resulting in the transformation of micelles into vesicles by the penetration of the HC chains into vesicle bilayers. To enable the HC chains to penetrate the vesicle bilayers, they may be bent. The increase in the number of gauche conformers in the HC chains inferred from the IR measurements indicates that the HC chains are indeed bent.

We also measured the electrical conductivity and the diffusion coefficients, D_{agg}, for the 10 mM F6H5OS solutions aged for 53 days at different concentrations (Figures S1 and S4, Supporting Information). The slope of the conductivity changed abruptly at 5.5 mM (Figure S4), and the D_{agg} values decreased beyond 5.5 mM (Figure S1), indicating that the micelle−vesicle transformation concentration for the aged solution was the same as that of the fresh solution. Whereas there were no differences in the D_{agg} values between the fresh and aged solutions below 5.5 mM, the D_{agg} value of the aged solution was smaller than that of the fresh solution (Figure S1). This result is consistent with the aforementioned consideration that F6H5OS kinetically forms micelles above the micelle−vesicle transition concentration (5.5 mM) immediately after the preparation of the solution, and subsequently aging makes the solution thermodynamically stable, transforming small micelles coexisting with vesicles to large aggregates (vesicles).

Conclusions

We studied changes in the morphology of aggregates formed by a hybrid surfactant, F6H5OS, in aqueous solution with time and the concentration. F6H5OS exhibited micelle−vesicle transition at 5.5 mM in water. Even though the aqueous solutions above the concentration of 5.5 mM contained a number of small micelles immediately after their preparation, the aging of the solution brought about the transformation of micelles into vesicles. Above the concentration of 5.5 mM, F6H5OS tended to kinetically form micelles, and the micelles subsequently transformed into vesicles with time. This unusual morphological change is related to the difference in hydrophobicity between the HC and FC chains in F6H5OS and to the mutual immiscibility of the FC and HC chains.

Supporting Information Available: Change in the D_{agg} values of fresh and aged F6H5OS solutions with surfactant concentrations (Figure S1). Contour plots constructed from data obtained in the 2D $^1H-^1H$ NOESY experiment involving the use of 10 mM fresh F6H5OS solution (Figure S2). The relation between the electrical conductivity of aqueous F6H5OS solutions containing 10 mM NaCl and surfactant concentrations (Figure S3). The relation between the electrical conductivity of aqueous aged F6H5OS solutions and surfactant concentrations (Figure S4). This information is available free of charge via the Internet at http://pubs.acs.org.

Acknowledgment. This work was supported by JSPS (Japan Society for the Promotion of Science) Core-to-Core Program (Advanced Particle Handling Science), and the electron microscopy work was performed at the Technion Soft Matter Electron Microscopy Laboratory with partial financial support from the Technion Russell Berrie Nanotechnology Institute (RBNI).

References and Notes

(1) Kaler, E.; Murthy, A.; Rodriguez, B.; Zasadzinski, J. *Science* **1989**, *245* (4924), 1371–1374.
(2) Kawasaki, H.; Imahayashi, R.; Tanaka, S.; Almgren, M.; Karlsson, G.; Maeda, H. *J. Phys. Chem. B* **2003**, *107* (33), 8661–8668.
(3) Mao, M.; Huang, J.; Zhu, B.; Yin, H.; Fu, H. *Langmuir* **2002**, *18* (8), 3380–3382.
(4) Shankar, B. V.; Patnaik, A. *Langmuir* **2007**, *23* (7), 3523–3529.
(5) Zhai, L.; Zhang, J.; Shi, Q.; Chen, W.; Zhao, M. *J. Colloid Interface Sci.* **2005**, *284* (2), 698–703.
(6) Gonzalez, Y. I.; Nakanishi, H.; Stjerndahl, M.; Kaler, E. W. *J. Phys. Chem. B* **2005**, *109* (23), 11675–11682.
(7) Johnsson, M.; Wagenaar, A.; Engberts, J. B. F. N. *J. Am. Chem. Soc.* **2003**, *125* (3), 757–760.
(8) Davies, T. S.; Ketner, A. M.; Raghavan, S. R. *J. Am. Chem. Soc.* **2006**, *128* (20), 6669–6675.
(9) Buwalda, R. T.; Stuart, M. C. A.; Engberts, J. B. F. N. *Langmuir* **2000**, *16* (17), 6780–6786.

(10) Kondo, Y.; Uchiyama, H.; Yoshino, N.; Nishiyama, K.; Abe, M. *Langmuir* **2002**, *11* (7), 2380–2384.
(11) Mendes, E.; Oda, R.; Manohar, C.; Narayanan, J. *J. Phys. Chem. B* **1998**, *102* (2), 338–343.
(12) Zheng, Y.; Lin, Z.; Zakin, J. L.; Talmon, Y.; Davis, H. T.; Scriven, L. E. *J. Phys. Chem. B* **2000**, *104* (22), 5263–5271.
(13) Battersby, B. J.; Lawrie, G. A.; Barnes, G. T. *Colloid Surf., B* **1999**, *13* (4), 179–185.
(14) Lu, T.; Han, F.; Li, Z.; Huang, J.; Fu, H. *Langmuir* **2006**, *22* (5), 2045–2049.
(15) Aydogan, N.; Aldis, N. *Langmuir* **2006**, *22* (5), 2028–2033.
(16) Calik, P.; Ileri, N.; Erdinc, B. I.; Aydogan, N.; Argun, M. *Langmuir* **2005**, *21* (19), 8613–8619.
(17) Kondo, Y.; Yoshino, N. *Curr. Opin. Colloid Interface Sci.* **2005**, *10* (3−4), 88–93.
(18) Yoshino, N.; Hamano, K.; Omiya, Y.; Kondo, Y.; Ito, A.; Abe, M. *Langmuir* **1995**, *11* (2), 466–469.
(19) Ito, A.; Kamogawa, K.; Sakai, H.; Hamano, K.; Kondo, Y.; Yoshino, N.; Abe, M. *Langmuir* **1997**, *13* (11), 2935–2942.
(20) Kondo, Y.; Miyazawa, H.; Sakai, H.; Abe, M.; Yoshino, N. *J. Am. Chem. Soc.* **2002**, *124* (23), 6516–6517.
(21) Miyazawa, H.; Igawa, K.; Kondo, Y.; Yoshino, N. *J. Fluorine Chem.* **2003**, *124* (2), 189–196.
(22) Braun, S.; Kalinowski, H.-O.; Berger, S. *150 and More Basic NMR Experiments*; Wiley-VCH: Weinheim, 1998; p 442.
(23) Holz, M.; Weingartner, H. *J. Magn. Reson.* **1991**, *92* (1), 115–125.
(24) Danino, D.; Talmon, Y.; Zana, R. *J. Colloid Interface Sci.* **1997**, *185* (1), 84–93.
(25) Li, Z.; Kesselman, E.; Talmon, Y.; Hillmyer, M. A.; Lodge, T. P. *Science* **2004**, *306* (5693), 98–101.
(26) Unsal, H.; Aydogan, N. *Langmuir* **2009**, *25* (14), 7884–7891.
(27) Israelachvili, J. N. *Intermolecular and Surface Forces*; Academic Press: London, 1985; Chapter 16.
(28) Amato, M. E.; Caponetti, E.; Martino, D. C.; Pedone, L. *J. Phys. Chem. B* **2003**, *107* (37), 10048–10056.
(29) MacPhail, R. A.; Strauss, H. L.; Snyder, R. G.; Elliger, C. A. *J. Phys. Chem.* **1984**, *88* (3), 334–341.
(30) Snyder, R. G.; Strauss, H. L.; Elliger, C. A. *J. Phys. Chem.* **1982**, *86* (26), 5145–5150.

JP1028273